

Measurement of the local Jahn-Teller distortion in $\text{LaMnO}_{3.006}$

Th. Proffen, R. G. DiFrancesco, S. J. L. Billinge

*Department of Physics and Astronomy and Center for Fundamental Materials Research,
Michigan State University, East Lansing, Michigan 48824-1116.*

E. L. Brosha and G. H. Kwei

Los Alamos National Laboratory, Los Alamos, New Mexico 87545.

(March, 4, 1999)

The atomic pair distribution function (PDF) of stoichiometric LaMnO_3 has been measured. This has been fit with a structural model to extract the *local* Jahn-Teller distortion for an ideal Mn^{3+}O_6 octahedron. These results are compared to Rietveld refinements of the same data which give the *average* structure. Since the *local* structure is being measured in the PDF there is no assumption of long-range orbital order and the real, local, Jahn-Teller distortion is measured directly. We find good agreement both with published crystallographic results and our own Rietveld refinements suggesting that in an accurately stoichiometric material there is long range orbital order as expected. The local Jahn-Teller distortion has 2 short, 2 medium and 2 long bonds. This implies that there is some mixing of the $d_{3z^2-r^2}$ and $d_{x^2-y^2}$ states and the occupied state is not pure $d_{3z^2-r^2}$ symmetry. The Debye temperature of the Mn and O ions has also been calculated as $\Theta_D(\text{Mn}) = 1000 \pm 100$ K, $\Theta_D(\text{O}_{\text{apical}}) = 980 \pm 30$ K and $\Theta_D(\text{O}_{\text{basal}}) = 601 \pm 8$ K.

I. INTRODUCTION

The Jahn-Teller (JT) distortion of the MnO_6 octahedra in perovskite manganites is known to have a significant effect on their electrical and magnetic properties. The JT distortion takes the form of an elongation of the octahedra. The simplest type of distortion is one in which the octahedra elongate along the direction of the $d_{3z^2-r^2}$ orbitals and contract in directions in which the $d_{x^2-y^2}$ orbitals point.¹ This distortion would give rise to 2 long Mn-O bonds and 4 short Mn-O bonds in each distorted octahedron. However, it is possible to generate a symmetry lowering distortion with a different symmetry by making some linear combination of the pure $d_{3z^2-r^2}$ and $d_{x^2-y^2}$ states. Because of the importance of the Jahn-Teller distortion in these materials it is critical to characterize the exact nature of the JT state in the manganites.

The MnO_6 octahedra pack together in space in a 3-dimensional corner shared network giving rise to the well-known perovskite structure. In general the distorted octahedra can be orientationally ordered (so-called orbital ordering) or disordered. If the orbitals are long-range ordered then a solution of the average crystal structure, as obtained from Rietveld refinement for example, will give the local bond-lengths in the octahedra accurately and reveal the nature of the local JT distortion. However, if the orbitals are not perfectly long-range ordered, the average crystal structure will not give the right result for the local JT distortion. However, a local structural probe such as extended x-ray absorption fine structure (XAFS) or the atomic pair distribution function (PDF) method, will still reveal the nature of the local distortion regardless of whether the orbitals are ordered or not.

Any determination of the nature of the local JT distortion using a crystallographic approach necessarily pre-

sumes perfect orbital order. This is thought to be good in the case of undoped LaMnO_3 where every manganese ion is in the 3+ state. However, by measuring the local structure directly using the PDF method, we do not make this presumption. We have measured the local JT distortion in a sample of composition $\text{LaMnO}_{3.006}$ using the PDF analysis of neutron powder diffraction data. The PDFs we measure are essentially sample, and not resolution, limited and the short and long bonds in the distorted MnO_6 octahedra are clearly resolved. These PDFs have been modelled using a full-profile least-squares refinement approach. These results are compared to crystallographic Rietveld refinements on the same data. We find excellent agreement for the Jahn-Teller distortion between the PDF and crystallographic analyses.

The average crystal structure of undoped LaMnO_3 has been extensively studied since the 1950's.²⁻¹¹ Differences between these studies occur largely because of the sensitivity of the structure to the sample stoichiometry which depends on synthesis conditions.⁹ It appears fairly widely accepted now that the correct structure for stoichiometric LaMnO_3 at low temperature is orthorhombic (space group $Pbnm$ or $Pnma$ depending on convention). The data assigned to a monoclinic space group by Mitchell *et al.*⁹ can be well refined in the orthorhombic space group as well with fewer degrees of freedom.¹¹ An excellent summary of the situation is presented in Rodriguez-Carvajal *et al.*¹¹ In this structure the long $d_{3z^2-r^2}$ orbitals lie in the same (basal) plane in a checkerboard type of arrangement so the bonds are long-short-long-short as you move from Mn to Mn along the Mn-O-Mn bond. Since all the long bonds lie in this plane, the separation of the Mn ions in the perpendicular direction (c -axis in the $Pbnm$ setting and b axis in the $Pnma$ setting) is shorter. This is the O' structure in the Goodenough specification.¹²

There is one report of a PDF measurement on the un-

doped LaMnO_3 material.¹³ In this case the monoclinic structure of Mitchell *et al.*⁹ was successfully fit to the data. However, no structural parameters were published. In this paper we publish the local structure parameters of LaMnO_3 determined from PDF data. The results are compared to a Rietveld refinement of the same data-set. There is excellent agreement between the average and the local structures indicating that the sample is fully long-range ordered. We find that, even locally, there is a significant orthorhombic distortion to the MnO_6 octahedra.

II. EXPERIMENTAL

The $\text{LaMnO}_{3+\delta}$ sample was prepared using standard solid state reaction methods. Stoichiometric amounts of La_2O_3 (Alfa Aesar Reacton 99.99%) and MnO_2 (Alfa Aesar Puratronic 99.999%) were ground in an Al_2O_3 mortar and pestle under acetone until well mixed. The powder sample was loaded into a 3/4" diameter die and uniaxially pressed at 1000 lbs. The pellet was placed into an Al_2O_3 boat and fired under pure oxygen for 12 hours at 1200-1250 °C. The sample was cooled to 800 °C and removed, reground, repelletized, and refired at 1200-1250 °C for an additional 24 hours. This process was repeated until a single phase, rhombohedral, x-ray diffraction pattern was obtained. Total reaction time was approximately 5 days. Thermogravimetric analysis (TGA) indicated that the as-prepared sample had an oxygen stoichiometry of about $\text{LaMnO}_{3.10}$.

The $\text{LaMnO}_{3.10}$ sample was ground, left in powder form, and placed into an Al_2O_3 boat. The sample was post-annealed in ultra high purity Ar at 1000 °C for 24 hours then quenched to room temperature. The oxygen stoichiometry was again determined using TGA under forming gas. The final oxygen stoichiometry was 3.006.

Neutron powder diffraction data were collected on the SEPD diffractometer at the Intense Pulsed Neutron Source (IPNS) at Argonne National Laboratory. The sample of about 10 g was sealed in a cylindrical vanadium tube with helium exchange gas. Data were collected at 20K in a closed cycle helium refrigerator. The data are corrected for detector deadtime and efficiency, background, absorption, multiple scattering, inelasticity effects and normalized by the incident flux and the total sample scattering cross-section to yield the total scattering structure function, $S(Q)$. This is Fourier transformed according to

$$G(r) = \frac{2}{\pi} \int_0^\infty Q[S(Q) - 1] \sin(Qr) dQ. \quad (1)$$

Data collection and analysis procedures have been described elsewhere.¹⁴ The reduced structure factor $F(Q) = Q[S(Q) - 1]$ is shown in Figure 1.

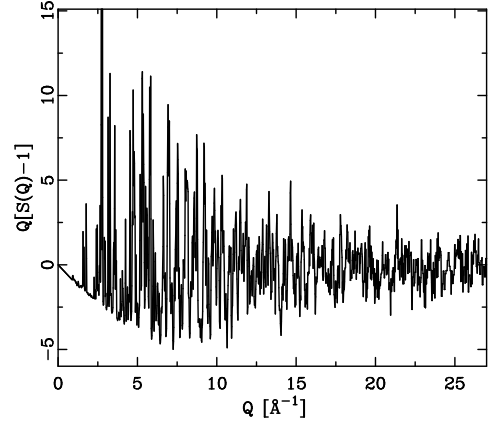


FIG. 1. Reduced structure factor $F(Q) = Q[S(Q) - 1]$ for LaMnO_3 measured at 10 K. The maximum value of $F(Q)$ is 26.

III. MODELLING AND RESULTS

The Rietveld refinements were carried out using the GSAS Rietveld code.¹⁵ Modelling of PDF was carried out using a least-squares full-profile PDF fitting procedure. This is exactly analogous to the Rietveld method except that the PDF is fit (in real-space) rather than the reciprocal-space data. When the PDF is fit the short-range order is obtained directly.¹⁶ The program we use is called PDFFIT. It is described in detail elsewhere and is available on request.¹⁷ The structural inputs for the program are atomic positions, occupancies and thermal factors.

The results are shown in Table I. We chose the convention used in Ref. 11 of putting Mn on the $(0, \frac{1}{2}, 0)$ position. Two PDF refinements are reported labelled A and B. The difference is the range of r over which the fit was made: A was made over a range $1.5 \text{ \AA} < r < 15.5 \text{ \AA}$; B over a range $1.5 \text{ \AA} < r < 3.5 \text{ \AA}$. Both refinements were constrained to have the symmetry of the $Pbnm$ space group. In addition, PDF-refinements were carried out where the space group symmetry was relaxed. However, the results of these refinements essentially reproduced those within the $Pbnm$ space group and the results are not reported here.

Of particular interest are the resulting MnO bond lengths in the MnO_6 octahedra, listed in Table II. The R-values given in Table II are calculated over the same interval 1.5 to 3.5 Å so they can be directly compared with each other. The observed and calculated PDFs for runs A and B are shown in Figure 2.

In addition, we have determined the Debye Temperature of the Mn and Oxygen ions from the refinements. The data were collected at 20 K. Assuming this is close enough to 0 K we use the expression

	Rietveld	Refinement A	Refinement B
a	5.542(1)	5.5422(7)	5.557(1)
b	5.732(1)	5.7437(8)	5.774(1)
c	7.6832(2)	7.690(1)	7.712(2)
x(La)	-0.0068(3)	-0.0073(2)	-0.0068(2)
y(La)	0.0501(3)	0.0488(2)	0.0504(1)
$\langle u^2 \rangle$ (La)	0.0022(4)	0.00199(4)	0.00177(4)
$\langle u^2 \rangle$ (Mn)	0.0011(6)	0.00067(7)	0.00071(7)
x(O1)	0.0746(4)	0.0729(3)	0.0734(2)
y(O1)	0.4873(4)	0.4857(3)	0.4800(2)
$\langle u^2 \rangle$ (O1)	0.0031(5)	0.00233(7)	0.00178(5)
x(O2)	0.7243(3)	0.7247(3)	0.7232(2)
y(O2)	0.3040(3)	0.3068(3)	0.3060(1)
z(O2)	0.0390(2)	0.0388(3)	0.0369(2)
$\langle u^2 \rangle$ (O2)	0.0030(4)	0.00378(5)	0.00439(4)
R_{wp}	12.1	16.2	9.1

TABLE I. Structural data of LaMnO_3 ($Pbnm$) from the Rietveld refinement and PDF refinements A and B. La and O1 are on $(x, y, \frac{1}{4})$, Mn is on $(0, \frac{1}{2}, 0)$ and O2 is on (x, y, z) . The units for the lattice parameters are \AA and for values of $\langle u^2 \rangle$ \AA^2 . The numbers in parentheses are the estimated standard deviation on the last digit.

Run	Mn-O (<i>s</i>)	Mn-O (<i>m</i>)	Mn-O (<i>l</i>)	R_{wp}
Rietveld	1.9200(3)	1.9662(4)	2.1609(4)	-
A	1.910(3)	1.9662(8)	2.178(3)	13.1
B	1.924(2)	1.9742(9)	2.177(2)	9.1

TABLE II. Mn-O bond lengths in units of \AA . For details see text.

$$\Theta_D = \frac{3h^2}{16\pi^2 m k_b \langle u^2 \rangle} \quad (2)$$

to determine the Θ_D from the refined thermal displacements, $\langle u^2 \rangle$ of Mn and O atoms, here m is the mass of the corresponding atom and k_b Boltzmann's constant. Thermal factors obtained from PDF refinements are often more accurate than Rietveld thermal factors because of the wider range of Q over which data are analyzed¹⁸. For example, in this study the PDF's were obtained from data collected up to $Q_{max} = 27 \text{ \AA}^{-1}$. This is almost double the Q -range used ($Q_{max} = 15.7 \text{ \AA}^{-1}$) in the Rietveld refinement of the same data. The Rietveld refinement was confined to a lower Q -range due to Bragg-peak overlap in the high- Q region. We have previously shown that the PDF can give accurate absolute values of Θ_D ¹⁹. The values we obtain are $\Theta_D(\text{Mn}) = 1000 \pm 100 \text{ K}$, $\Theta_D(\text{O1}) = 980 \pm 30 \text{ K}$ and $\Theta_D(\text{O2}) = 601 \pm 8 \text{ K}$.

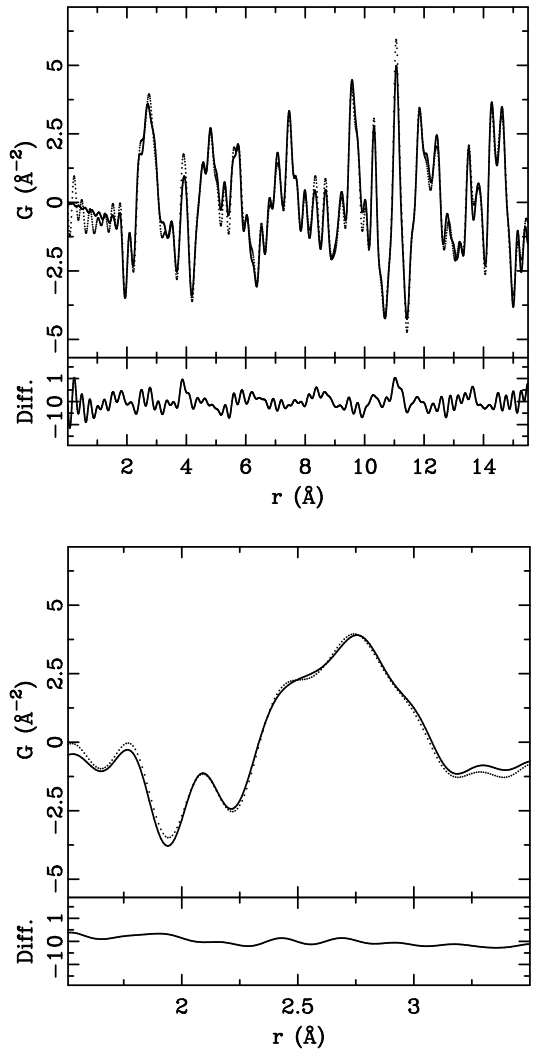


FIG. 2. Experimental PDF (circles) and model PDF (solid line) for refinements A (top) and B (bottom). Difference curves are plotted below the data.

IV. DISCUSSION

The average crystallographic structure suggests that the Jahn-Teller distorted octahedra in LaMnO_3 contain two short (*s*) bonds (1.9200 \AA), two less short (*m*) bonds (1.9662 \AA) and two long (*l*) bonds (2.1609 \AA). The PDF peaks corresponding to these Mn-O bonds can be seen in Fig. 2 at around $r = 2 \text{ \AA}$ as negative peaks.²⁰ A double-peak structure is clearly resolved reflecting the high resolution of the PDF measurement.

The motivation for this study was to determine whether the real, local, JT distorted octahedra had 4-*s* and 2-*l* bonds (pure Q_3 distortion²¹), which one would expect for an isolated octahedron, or 2-*s*, 2-*m* and 2-*l* bonds (some Q_2 component) as suggested by the average structure. The JT distorted octahedra could be locally Q_3 but appear further distorted in the average structure if there was some orbital disorder (for example,

some of the long bonds orienting parallel to the c -axis). These two scenarios can be distinguished in a joint Rietveld/PDF study where the average and local structures are determined from the same data-set.

When the PDF is fit over a wide r -range (run A) the Mn-O bond lengths are similar to the Rietveld values, suggesting that the local bond-length distribution matches that of the average structure. However, it is possible that even by $r = 15$ Å the effects of possible orbital disorder will bias the results of the PDF refinement towards the average values. To check this, we carried out run B which fits only over the range to 3.5 Å. This PDF-range contains only the MnO_6 octahedra themselves and does not depend on how they are oriented in space. It is clear from Table II that the refinement still prefers two short, two less-short and two long bonds. As a final check we carried out refinements where the $Pbnm$ space-group symmetry was relaxed so that all Mn and O ion positions can vary independently. This allows up to six different Mn-O bond-lengths to refine within one octahedron. The refinements again resulted in the bond lengths grouping into 2 short, 2 less short and 2 long. It is clear that the PDF peak corresponding to the short octahedral bonds is broader than can be explained by a single Mn-O bond-length. This is strong evidence that the local Jahn-Teller distortion is not a pure stretch of the $d_{3z^2-r^2}$ orbitals but there is a small amount of $d_{x^2-y^2}$ character mixed in and there is some Q_2 character to the static distortion.

This can be explained by the fact that the *average* structure is orthorhombic and so the octahedra are sitting in an orthorhombic crystal field. It is helpful to understand the origin of the long-range orthorhombicity of the structure itself. This comes about because of the rotations (about $\langle 111 \rangle$ directions) of the corner-shared octahedra. This does not in itself result in an orthorhombic distortion; however, if the octahedra themselves are elongated and the orbitals ordered, as in this case, an orthorhombic distortion does result. The basal-plane distortion $(2(a-b)/(a+b))$ where a refers to the axis of the orthorhombic cell) is explained straightforwardly by reference to Fig. 3(b). In this figure the octahedra are shown elongated and it is clear how the rotations give rise to the basal plane distortion.

The manganese-manganese separation along the perpendicular direction is also different to the basal plane, but this is due to a different reason. With the pattern of orbital ordering in this O' structure, all of the long Mn-O bonds lie in the basal plane and all the Mn-O bonds along the c -direction are short. The separation of manganese ions along the c direction is therefore shorter than in the basal plane and $c/\sqrt{2} \leq a \leq b$. This would still hold if the shapes of the octahedra themselves were tetragonal (pure Q_3 distortion) and comes simply from the fact that the long bonds all lie in the basal plane. Thus, the structure could accommodate having tetragonally (Q_3) distorted octahedra within the orthorhombic unit cell by choosing the appropriate c -axis lattice parameter to make the Mn-O(2) bond along the c -direction the same as the Mn-O(1)

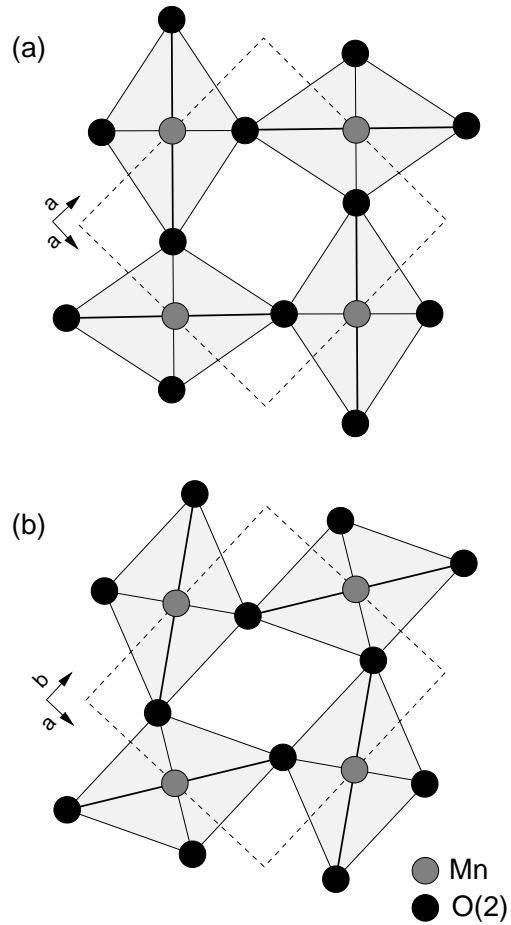


FIG. 3. Schematic drawing of the arrangement of MnO_6 octahedra projected down the c -axis. The long distance in the octahedra corresponds to the $d_{3z^2-r^2}$ orbital, the short distance to $d_{x^2-y^2}$. (a) the octahedral rotations have been set to zero resulting in a square based unit cell ($a = b$). (b) Finite rotations result in the orthorhombic structure ($a \neq b$) that is observed.

(in-plane) short bond. In fact this does not happen.

What is clear from the local Mn-O bond-lengths is that there is a large Q_3 distortion with a small Q_2 distortion superimposed. The large Q_3 distortion breaks the degeneracy of the e_g orbitals and separates them widely in energy (~ 0.5 eV).²² The additional small Q_2 distortion comes about by mixing the pure $d_{3z^2-r^2}$ and $d_{x^2-y^2}$ but is presumably a small response of the local octahedra to the orthorhombic crystal field, even though this long-range orthorhombicity results from the large local Q_3 distorted octahedra (and their rotations).

V. CONCLUSIONS

We have fit a high-resolution atomic pair distribution function obtained from powder neutron diffraction data to determine the local Jahn-Teller distortion in stoichio-

metric LaMnO_3 . We observe a small but significant difference in the length of the in-plane ($1.924(2)$ Å) and out-of plane ($1.9742(9)$ Å) short bonds, and a well separated long bond ($2.177(2)$ Å). This implies that there is some mixing of the $d_{3z^2-r^2}$ and $d_{x^2-y^2}$ levels and the occupied e_g state is not pure $d_{3z^2-r^2}$ in character. This is in agreement with the result from crystallography; however, it is important to determine this directly from the local structure as we report here since any orbital disorder (for example, due to small non-stoichiometries) would affect the crystal structure but not the local structure. Finally, we report estimates of the Debye temperature of Mn and O ions in this compound.

ACKNOWLEDGMENTS

We would like to acknowledge stimulating discussions with S. D. Mahanti, P. Radaelli and T. A. Kaplan. This work was supported by the NSF through grant DMR-9700966 at MSU and the DOE through contract W-7405-ENG-36 at LANL. The IPNS is funded by the U.S. Department of Energy under Contract W-31-109-Eng-38.

- ¹⁴ S. J. L. Billinge and T. Egami, Phys. Rev. B **47**, 14386 (1993).
- ¹⁵ A. C. Larson and R. B. Von Dreele, General structure analysis system, Report No. LAUR-86-748, Los Alamos National Laboratory, Los Alamos, NM 87545, 1987.
- ¹⁶ S. J. L. Billinge, in *Physics of Manganites*, edited by T. A. Kaplan and S. D. Mahanti, page 201, New York, 1999, Plenum.
- ¹⁷ Th. Proffen and S. J. L. Billinge, J. Appl. Cryst. (1999), in press.
- ¹⁸ S. J. L. Billinge, in *Local Structure from Diffraction*, edited by S. J. L. Billinge and M. F. Thorpe, page 137, New York, 1998, Plenum.
- ¹⁹ I-K. Jeong, Th. Proffen, F. Mohiuddin-Jacobs, and S. J. L. Billinge, **103**, 921 (1999).
- ²⁰ The PDF peak originating from the pair of atoms i and j is weighted by the product $b_i b_j$ where b_i is the scattering length of atom i . Since the neutron scattering length of Mn is negative, the Mn-O peaks in the PDF are negative.
- ²¹ M. D. Sturge, in *Solid State Physics*, edited by F. Seitz, D. Turnbull, and H. Ehrenreich, volume 20, New York, 1967, Academic.
- ²² A. J. Millis, P. B. Littlewood, and B. I. Shraiman, Phys. Rev. Lett. **74**, 5144 (1995).

-
- ¹ J. S. Griffith, *The Theory of Transition Metal Ions*, Cambridge University Press, Cambridge, 1964.
 - ² A. Wold and R. Arnott, J. Phys. Chem. solids **3**, 238 (1959).
 - ³ E. O. Wollan and W. C. Koehler, Phys. Rev. **100**, 545 (1955).
 - ⁴ J. B. A. A. Elemans, B. Van Laar, K. R. Van Der Veen, and B. O. Loopstra, J. Solid State Chem. **3**, 238 (1971).
 - ⁵ B. C. Tofield and W. R. Scott, J. Solid State Chem. **10**, 183 (1974).
 - ⁶ J. A. M. van Roosmalen and E. H. P. Cordfunke, J. Solid State Chem. **93**, 212 (1991).
 - ⁷ J. A. M. van Roosmalen, E. H. P. Cordfunke, R. B. Helmholdt, and H. W. Zandbergen, J. Solid State Chem. **110**, 100 (1994).
 - ⁸ P. Norby, I. G. K. Andersen, E. K. Andersen, and N. H. Andersen, J. Solid State Chem. **119**, 191 (1995).
 - ⁹ J. F. Mitchell, D. N. Argyriou, C. D. Potter, D. G. Hinks, J. D. Jorgensen, and S. D. Bader, Phys. Rev. B **54**, 6172 (1996).
 - ¹⁰ Q. Huang, A. Santoro, J. W. Lynn, R. W. Erwin, J. A. Borchers, J. L. Peng, and R. L. Greene, Phys. Rev. B **55**, 14987 (1997).
 - ¹¹ J. Rodríguez-Carvajal, M. Hennion, F. Moussa, A. H. Moudden, L. Pinsard, and A. Revcolevschi, Phys. Rev. B **57**, R3189 (1998).
 - ¹² J. B. Goodenough, Phys. Rev. **100**, 564 (1955).
 - ¹³ D. Louca, T. Egami, E. L. Brosha, H. Röder, and A. R. Bishop, Phys. Rev. B **56**, R8475 (1997).